

ELECTRON-CAPTURE SUPERNOVAE AS ORIGIN OF ^{48}Ca SHINYA WANAJO¹, HANS-THOMAS JANKA², AND BERNHARD MÜLLER²*Draft version March 14, 2013*

ABSTRACT

We report that electron-capture supernovae (ECSNe), arising from collapsing oxygen-neon-magnesium cores, are a possible source of ^{48}Ca , whose origin has remained a long-standing puzzle. Our two-dimensional, self-consistent explosion model of an ECSN predicts ejection of neutron-rich matter with electron fractions $Y_e \approx 0.40\text{--}0.42$ and relatively low entropies, $s \approx 13\text{--}15 k_B$ per nucleon (k_B is the Boltzmann constant). Post-processing nucleosynthesis calculations result in appreciable production of ^{48}Ca in such neutron-rich and low-entropy matter during the quasi-nuclear equilibrium and subsequent freezeout phases. The amount of ejected ^{48}Ca can account for that in the solar inventory when we consider possible uncertainties in the entropies. ECSNe could thus be a site of ^{48}Ca production in addition to a hypothetical, rare class of high-density Type Ia supernovae.

Subject headings: nuclear reactions, nucleosynthesis, abundances — stars: abundances — supernovae: general

1. INTRODUCTION

The origin of the most neutron-rich (n-rich) stable isotope among the iron-group nuclei and lighter elements, ^{48}Ca , remains a long-standing mystery of nucleosynthesis (see Hartmann et al. 1985; Meyer et al. 1996, for the historical background). ^{48}Ca constitutes only 0.187% of the solar calcium abundance (Asplund et al. 2009), but is 47 times more abundant than its next heavier stable isotope, ^{46}Ca . From the point of view of nuclear stability, this can be attributed to the doubly magic structure of ^{48}Ca with $Z = 20$ and $N = 28$. Thermal equilibrium, such as nuclear statistical equilibrium (NSE) or quasi-nuclear equilibrium (QSE), thus seems to be responsible for the creation of ^{48}Ca , in which each isotopic abundance is a strong function of its binding energy per nucleon. Such a formation of ^{48}Ca demands a highly n-rich environment with Y_e (number of protons per nucleon) being close to that characterizing the structure of ^{48}Ca , $Y_{e,\text{nuc}} = 0.417$.

Hartmann et al. (1985) suggested n-rich NSE as the production mechanism of ^{48}Ca , based on the assumption that such conditions would be met in the innermost ejecta of core-collapse supernovae (CCSNe). Meyer et al. (1996) argued, however, that QSE was responsible for the creation of ^{48}Ca . They showed that a low-entropy environment, characterized by $\phi < 1$, led to the appreciable creation of ^{48}Ca , where $\phi \equiv 0.34 T_9^3 / \rho_5$ is the photon-to-nucleon ratio with T_9 being the temperature in 10^9 K and ρ_5 the matter density in 10^5 g cm⁻³. For this reason, Meyer et al. (1996) concluded that CCSNe were excluded as the origin of ^{48}Ca because of their high entropies ($\phi > 1$) in the neutrino-driven ejecta. Such a high ϕ leads to an α -rich freezeout from NSE (Woosley & Hoffman 1992; Meyer et al. 1998a) followed by QSE, in which nuclear stability prefers heavier nuclei than ^{48}Ca . Instead, they concluded Type Ia supernovae (SNe Ia) as the unique site that could achieve such low

ϕ environments. Woosley (1997) explored SN Ia models with a central density of $(4\text{--}8) \times 10^9$ g cm⁻³ (needed to obtain $Y_e \sim 0.40\text{--}0.42$), which was substantially higher than the typical values of about 2×10^9 g cm⁻³. He found the production of $^{48}\text{Ca}/^{56}\text{Fe}$ to be about 100 times larger than its solar ratio. Given the observational fact that about one half of the Galactic iron comes from SNe Ia (Timmes et al. 1995), Woosley (1997) estimated an event rate of such high-density explosions no more than a few percent of the observed SNe Ia rate.

In this Letter, we propose that electron-capture SNe (ECSNe), a sub-class of CCSNe arising from collapsing O-Ne-Mg cores, can be additional sites of ^{48}Ca production. A recent two-dimensional (2D), self-consistent simulation of an ECSN predicts the ejection of n-rich matter of $Y_e \sim 0.40\text{--}0.42$ with $s \sim 14 k_B/\text{nuc}$ (k_B is the Boltzmann constant; Janka et al. 2008, 2012; Wanajo et al. 2011). These entropies, or $\phi \sim 1.4$, are only slightly above the limit of the criterion for ^{48}Ca formation considered by Meyer et al. (1996). We utilize this ECSN model (§ 2) for nucleosynthesis calculations and discuss the production mechanism of ^{48}Ca (§ 3). The mass-integrated nucleosynthetic yields are then compared with the solar abundances to test if our ECSN model accounts for the ^{48}Ca abundance in the solar inventory (§ 4).

2. ECSN MODEL

The nucleosynthesis analysis makes use of about 2000 representative tracer particles, by which the thermodynamic histories of ejecta chunks were followed in our self-consistent 2D hydrodynamic calculation of an ECSN (Janka et al. 2008, 2012; Wanajo et al. 2011). The model was computed with a ray-by-ray-plus treatment of the energy-dependent neutrino transport (Rampp & Janka 2000; Buras et al. 2006; Kitaura et al. 2006). The pre-collapse model of the O-Ne-Mg core emerged from the evolution of an $8.8 M_\odot$ star (Nomoto 1987). In our model, a neutrino-powered explosion sets in at about 100 ms after core bounce with an energy of about 10^{50} erg (Janka et al. 2008). Because of the very steep density gradient near the core surface, an interesting amount of

¹ National Astronomical Observatory of Japan, 2-21-1 Osawa, Mitaka, Tokyo 181-8588, Japan; shinya.wanajo@nao.ac.jp

² Max-Planck-Institut für Astrophysik, Karl-Schwarzschild-Str. 1, D-85748 Garching, Germany

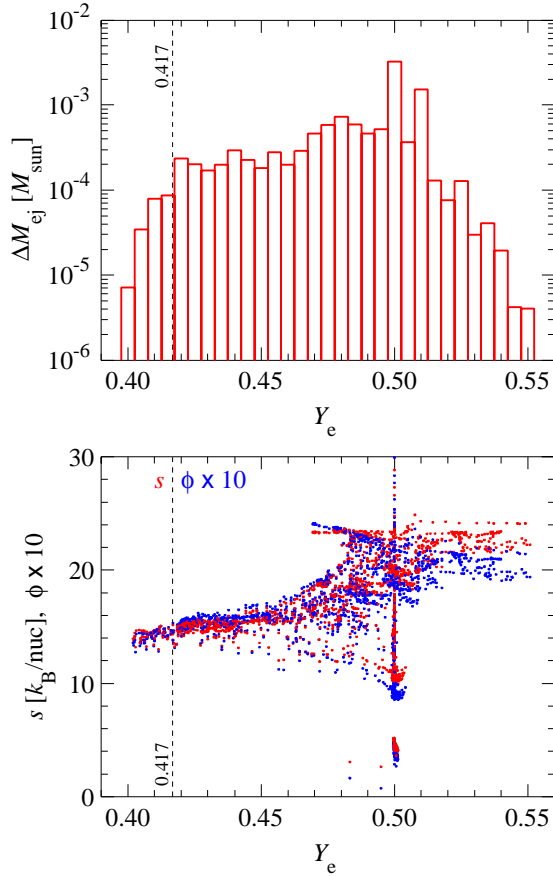


FIG. 1.— Top: Ejecta masses vs. Y_e at $T_9 = 5$ for our ECSN model. The width of the Y_e -bins is chosen to be $\Delta Y_e = 0.005$. The total ejecta mass from the core is $1.14 \times 10^{-2} M_\odot$. Also indicated by a dashed line is $Y_{e,\text{nuc}} = 0.417$. Bottom: s and ϕ as functions of Y_e at $T_9 = 5$ for all tracer particles.

n-rich matter with relatively low entropy ($s \approx 13\text{--}15 k_B$ for $Y_e < 0.42$) gets ejected (Figure 1; top)³. This happens only in the multi-dimensional case, which allows for the rapid expansion of neutrino-heated gas in buoyant, mushroom-like plumes, whose expansion is too rapid for ν_e and $\bar{\nu}_e$ absorptions to lift Y_e to values closer to 0.5, in contrast to the 1D case or more massive Fe-core progenitors, where the ejecta expansion is much slower and neutrino absorption proceeds longer. The entropies are lower for the lower Y_e particles as a result of less neutrino energy deposition. The photon-to-nucleon ratios (Fig. 1; bottom) are approximately one-tenth of the entropies, showing however a slightly steeper gradient for $Y_e < 0.42$. The expansion timescales of the particles, defined as the e -folding time of the temperature drop below 0.5 MeV, are $\tau_{\text{exp}} = 50\text{--}100$ ms and are largely independent of Y_e .

3. ^{48}Ca PRODUCTION

The nucleosynthetic yields are obtained with the reaction network code described in Wanajo et al. (2009, 2011) by employing the latest reaction library of REACLIB V2.0 (Cyburt et al. 2010). Using thermodynamic trajectories directly from the ECSN model, the calculations are started when the temperature decreases to

³ Y_e , s , and ϕ are those evaluated at $T_9 = 5$ throughout this paper.

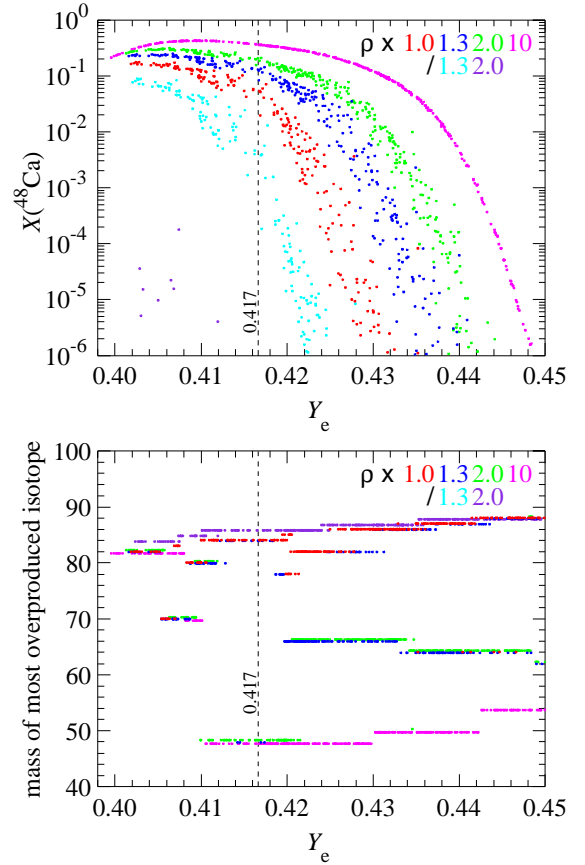


FIG. 2.— Top: Final mass fractions of ^{48}Ca for the tracer particles in the range of $Y_e < 0.45$. Also indicated by a dashed line is $Y_{e,\text{nuc}} = 0.417$. The result of the unchanged model is shown in red, and those with the densities multiplied by factors of 1.3, 2.0, 10 and divided by factors of 1.3, 2.0 are given in different colors. Bottom: Mass numbers of nuclei that have the greatest production factors (X/X_\odot) as functions of Y_e (slightly shifted in the vertical direction for visibility).

$T_9 = 10$, assuming initially free protons and neutrons with mass fractions $Y_{e,i}$ and $1 - Y_{e,i}$, respectively ($Y_{e,i}$ is the value at $T_9 = 10$).

The final mass fractions of ^{48}Ca for the tracer particles in the range of $Y_e < 0.45$ are shown as a function of Y_e by red dots in the upper-panel of Figure 2. We find appreciable production of ^{48}Ca in the range below its $Y_{e,\text{nuc}}$ (dashed line), peaking at $Y_e \approx 0.40$ ⁴. ^{48}Ca is always made as itself, its double-magic nature affording a special degree of stability in nuclear equilibrium.

To examine the nucleosynthesis of ^{48}Ca in detail, let us pick a representative tracer particle with $Y_e = 0.417$, $s = 14.3 k_B/\text{nuc}$ ($\phi = 1.45$), and $\tau_{\text{exp}} = 56.7$ ms. Note that the Y_e is slightly greater than $Y_{e,i} = 0.414$ as a result of neutrino reactions and the α -effect (McLaughlin et al. 1996; Meyer et al. 1998b). The abundances (defined by $Y \equiv X/A$; number per nucleon) of n, p, α , heavy nuclei ($Z > 2$), and ^{48}Ca are displayed as a function of descending temperature in panel of Figure 3 (upper-left). We find that the abundance of heavy nuclei is fixed around $T_9 = 6.24$. This is a consequence of the fact that the 3-body reactions $\alpha(\alpha\alpha, \gamma)^{12}\text{C}$ (hereafter

⁴ Test calculations with $Y_{e,\text{min}}$ replaced by even lower values result in the drop-off of $X(^{48}\text{Ca})$ around $Y_e \lesssim 0.390$.

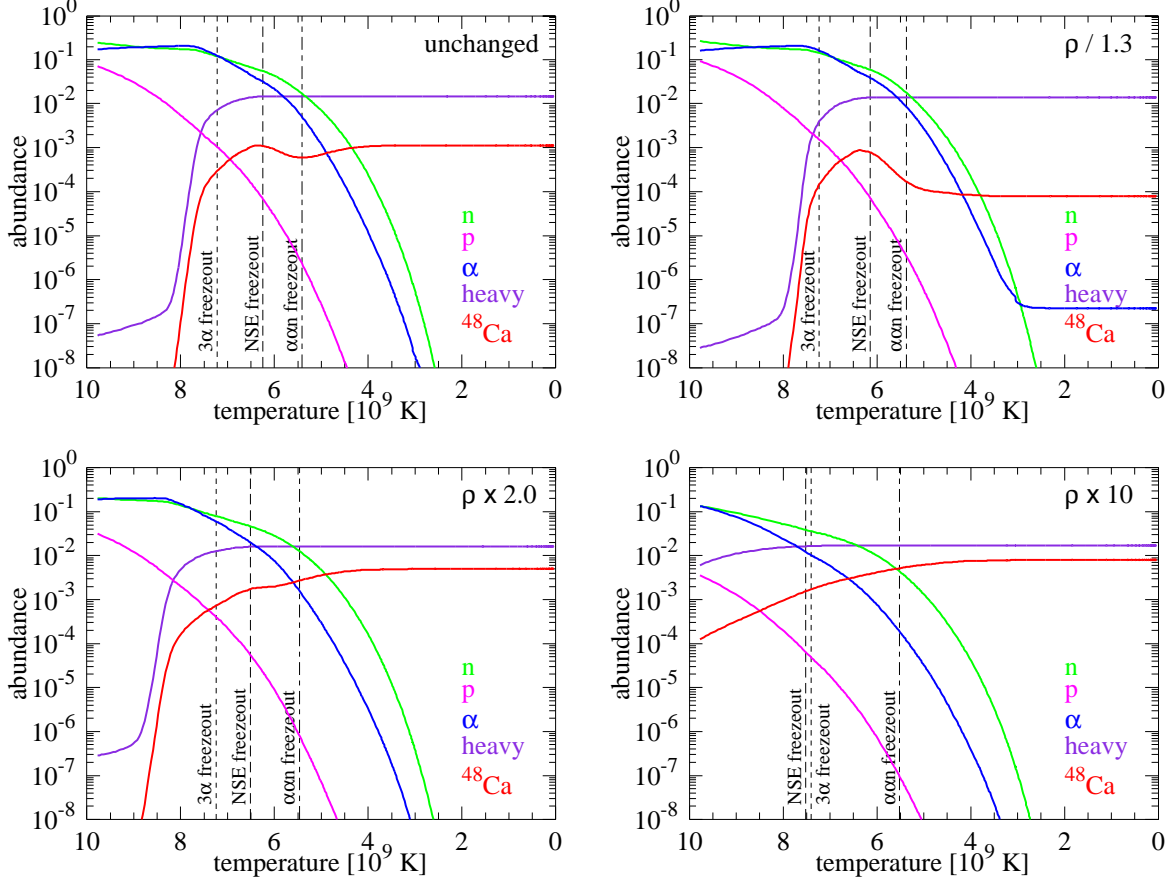


FIG. 3.— Abundances of n , p , α , heavy nuclei ($Z > 2$), and ^{48}Ca as functions of descending temperature for the tracer particle with $Y_e = 0.417$, $s = 14.3 k_B/\text{nuc}$ ($\phi = 1.45$), and $\tau_{\text{exp}} = 56.7$ ms. The result of the unchanged model is shown in the upper-left, and those for the densities divided by a factor of 1.3 and multiplied by factors of 2.0, 10 are shown in upper-right, lower-left, and lower-right panels, respectively. The long-dashed lines mark the NSE-freezeout temperatures. Also indicated by dashed and long-short-dashed lines are the temperatures at which the α -consumption timescales evaluated by 3α and $\alpha\alpha n$, respectively, become longer than τ_{exp} .

3α) and $\alpha(\alpha n, \gamma)^9\text{Be}$ followed by $^9\text{Be}(\alpha, n)\text{C}^{12}$ (hereafter $\alpha\alpha n$) become slow as the matter expands. The α -consumption timescale, $\tau_{3\alpha} \equiv -Y_\alpha/(dY_\alpha/dt)$ evaluated by 3α , first exceeds τ_{exp} at $T_9 = 7.22$ (dashed line). The gateway from light to heavy nuclei is closed when the timescale $\tau_{\alpha\alpha n}$ evaluated by $\alpha\alpha n$ as well exceeds τ_{exp} ($T_9 = 5.41$; long-short-dashed line). In general, NSE freezes between the 3α and $\alpha\alpha n$ freezeouts. We define the NSE-freezeout temperature ($T_9 = 6.24$; long-dashed line) at which the timescale of heavy abundance formation, $\tau_{\text{heavy}} \equiv Y_{\text{heavy}}/(dY_{\text{heavy}}/dt)$, exceeds τ_{exp} . Once the NSE freezes, the number of heavy nuclei in QSE cannot decrease because of their net photodisintegration being too slow (Meyer et al. 1996). The fixed number of heavy nuclei is in fact the key condition of QSE.

We find that the transition from NSE to QSE takes place with the number of α 's slightly greater than that of heavy nuclei. The abundances become redistributed by absorptions of light nuclei,⁵ decreasing the abundance of ^{48}Ca and increasing the abundances of heavier nuclei

⁵ In QSE, individual reactions, which are in general much faster than the expansion timescales of matter, are irrelevant. What determine the abundance distribution are nuclear binding energies per nucleon. Individual reactions play roles only after a freezeout from QSE ($T_9 \approx 4$; see § 4 in Meyer et al. 1998a). Note also that α 's are in nuclear equilibrium with free nucleons throughout the QSE phase. All n , p , α thus play roles for readjustment of the QSE abundances.

in the QSE cluster (Figure 4). In the late QSE phase ($T_9 \approx 5.5-4$), however, the ^{48}Ca abundance recovers in response to a drop-off of the α abundance. The number of charged light nuclei becomes insufficient to transmute ^{48}Ca into heavier nuclei. The abundance redistribution is predominantly due to photodisintegration and n -absorption, which cannot make a net upward shift in Z . Instead, ^{48}Ca increases in the local equilibrium around its double-magic intersection, lasting until the freezeout from QSE at $T_9 \approx 4$. In the end, however, the most abundant isotope is ^{66}Zn , the daughter of p -magic ^{66}Ni (Fig. 4).

How can we keep ^{48}Ca increasing in the QSE phase? Obviously, the presence of α 's is the cause of shifting light QSE abundances toward a greater Z in the above case. We thus test the sensitivity of the ^{48}Ca production to entropy, the key quantity that controls the α abundance. Figure 3 gives the results in which densities are divided by 1.3 (upper-right) or multiplied by 2.0 (lower-left), 10 (lower-right) throughout the calculations for the same tracer particle. The ϕ 's (and roughly s 's) decrease or increase by the inverse of the density scaling factor in each case. We find that the “ $\rho/1.3$ ” case ($\phi = 1.89$) leads to NSE freezeout with appreciably abundant α 's compared to heavy nuclei (hereafter α -rich QSE; $Y_\alpha/Y_{\text{heavy}} > 1$)⁶.

⁶ This is equivalent to a “QSE with too few heavy nuclei” com-

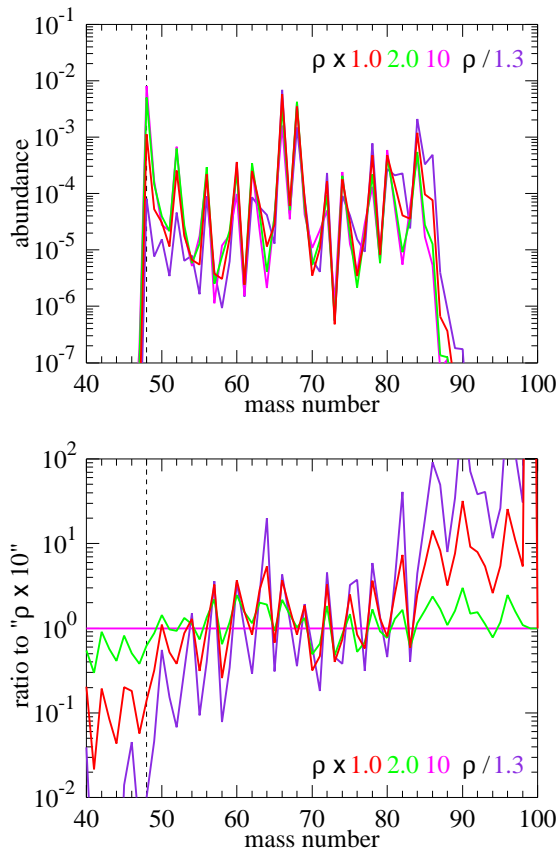


FIG. 4.— Final abundances as functions of mass number (upper panel) for the same tracer particle in Fig. 3. The result of the unchanged model is shown in red, and those for the densities divided by a factor of 1.3 or multiplied by factors of 2.0, 10 are shown in different colors. The position of ^{48}Ca is indicated by a dashed line. The abundance ratios relative to the “ $\rho \times 10$ ” case are also shown in the lower panel.

In this condition, light nuclei are so abundant that the ^{48}Ca abundance continuously decreases. In contrast, for the “ $\rho \times 2$ ” case ($\phi = 0.725$), the NSE freezes with a smaller α abundance that is comparable to that of heavy nuclei (hereafter α -poor QSE; $Y_\alpha/Y_{\text{heavy}} \lesssim 1$)⁷. Such low levels of charged light nuclei allow ^{48}Ca to continuously increase during QSE and even after the QSE freezeout by $T_9 \approx 2$. In fact, it is the most abundant isotope in the end (Fig. 4). The “ $\rho \times 10$ ” case ($\phi = 0.145$) gives a limiting condition of α -poor QSE, resulting in a robust ^{48}Ca creation. Figure 4 displays the final abundances for the same cases and those relative the “ $\rho \times 10$ ” case. From the lower panel, it is clearly seen that a more α -rich QSE tends to shift more abundances from lighter to heavier mass numbers. We conclude, therefore, that α -poor QSE is the mechanism for making ^{48}Ca as suggested by Meyer et al. (1996).

Figure 2 (top) shows the result of sensitivity tests with various density scaling factors for all the tracer particles. Overall, the synthesis of ^{48}Ca is quite sensitive to entropy (or ϕ) in the range $\phi \gtrsim 1$ as shown in Meyer et al. (1996). In the explored range, ^{48}Ca is more robustly produced

pared to what would be expected in NSE with the same density and temperature described in Meyer et al. (1996, 1998a).

⁷ This is equivalent to a “QSE with too many heavy nuclei” compared to NSE (Meyer et al. 1996, 1998a), in which QSE cannot reduce the number of heavy nuclei and thus ^{48}Ca survives.

in the more n-rich environment, $Y_e < Y_{e,\text{nuc}} = 0.417$. As an example, the particles with $Y_e \approx 0.402$ in the “ $\rho/1.3$ ” case have similar ^{48}Ca abundances to those of the unchanged case with $Y_e \approx 0.417$, despite larger ϕ ’s for the former (≈ 1.77) than the latter (≈ 1.44). This is a consequence of the $\alpha\alpha n$ reaction more rapid in more n-rich matter (Meyer et al. 1998a), leading to a faster consumption of α ’s. It is important to note, however, that ^{48}Ca is nowhere the most overproduced isotope (i.e., with the greatest X/X_\odot) in the explored range of our unchanged model as shown in Figure 2 (bottom). For $Y_e < 0.417$, ^{82}Se or ^{84}Kr are generally the most overproduced isotopes. Only the “ $\rho \times 2.0$ ” and “ $\rho \times 10$ ” cases, corresponding to $\phi \lesssim 0.7$, lead to the production of ^{48}Ca as the most overproduced isotope over a certain range in Y_e . In summary, the physical conditions of our ECSN model lie in the transition region between the α -rich ($\phi \gtrsim 1$) and α -poor ($\phi \lesssim 1$) QSEs (see Fig. 1 in Meyer et al. 1996).

4. CONTRIBUTION TO THE GALAXY

To examine whether ECSNe can be significant producers of ^{48}Ca in the Galaxy, the final abundances are obtained by mass integration over all the tracer particles. Figure 5 (upper-left) gives the isotopic mass fractions (after all radioactivities have decayed) relative to their solar values (Lodders 2003), i.e., the “production factors”, as a function of mass number for our unchanged model. The “normalization band” between the maximum (352 for ^{86}Kr) and one-tenth of that is indicated in yellow with the medium marked by a dashed line. Isotopes that fall into this band can be accepted as being made in considerable amounts by ECSNe. A reasonable “flatness” of production factors can be seen between $A \sim 60$ and 90, in which many isotopes fall into the normalization band. ^{48}Ca (shown by asterisk) is however located slightly below the normalization band. This implies that ECSNe contribute to the production of ^{48}Ca no more than 10% of its solar content.

As explored in § 3, the nucleosynthesis of ^{48}Ca is highly sensitive to entropy and our unchanged model appears to lie in the edge of the α -poor QSE condition. As a sensitivity test to entropy, the mass-integrated production factors for “ $\rho \times 1.3$ ”, “ $\rho \times 2.0$ ”, and “ $\rho \times 10$ ” are also displayed in the upper-right, lower-left, and lower-right panels of Figure 5, respectively. The result of “ $\rho \times 1.3$ ” satisfies the condition of ^{48}Ca being in the middle of the normalization band, which means that the model can account for one-third of ^{48}Ca in the solar system. In order to fully account for the origin of ^{48}Ca , one needs to increase the densities (that is equivalent to reduce ϕ ’s) by a factor of two (Fig. 5; lower-left). The reduced entropies lead to α -poor QSE conditions in a broad range of Y_e , in which ^{48}Ca is copiously produced (Figure 2; top). In fact, it is the most overproduced isotope for $0.41 \lesssim Y_e \lesssim 0.42$ in this case (Figure 2; bottom). ^{50}Ti and ^{54}Cr , the isotopes made in α -poor QSE, are also enhanced. The change here corresponds to a reduction of the entropies from $s \sim 14 k_B/\text{nuc}$ to $\sim 11 k_B/\text{nuc}$ or $\sim 7 k_B/\text{nuc}$ in the range $Y_e < 0.42$. This does not seem to be an extreme assumption, although the reduced values tend to scratch the lower end of the range of entropies that are compatible with neutrino-heated ejecta of EC-

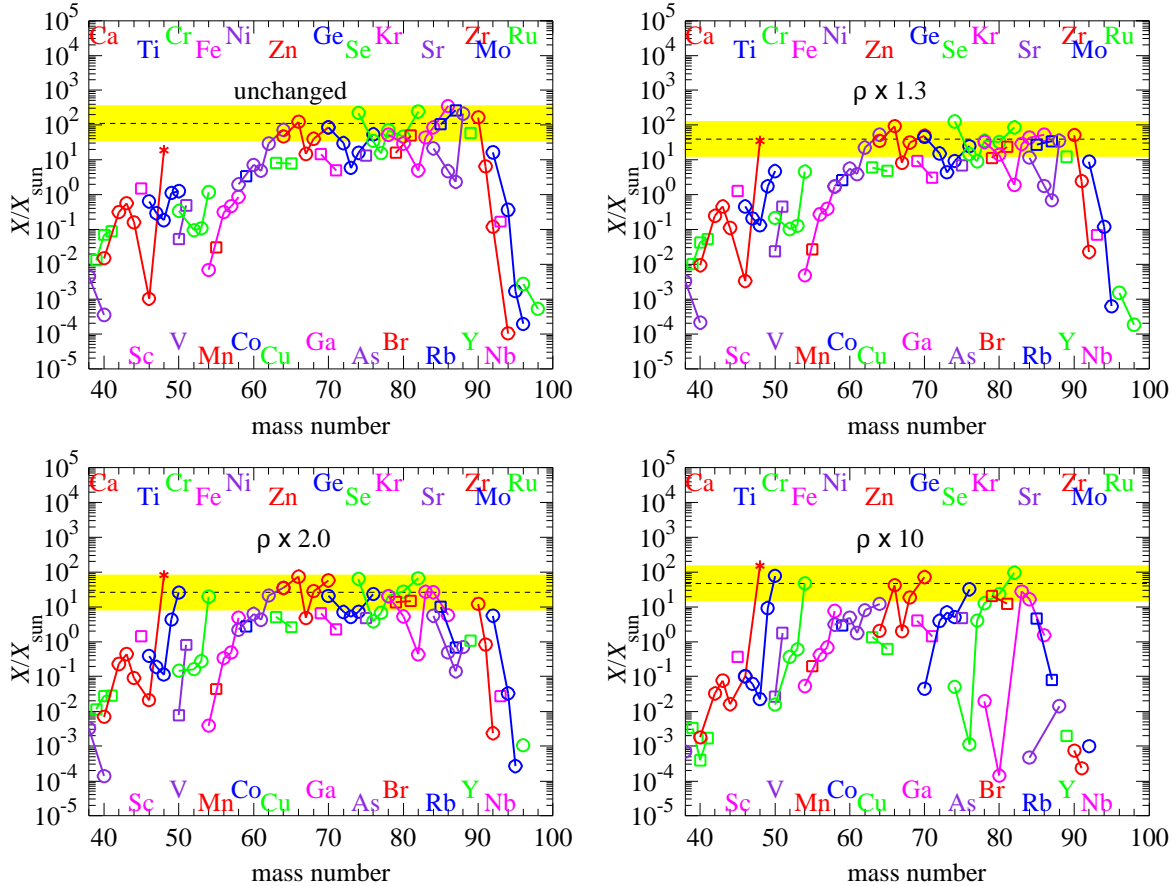


FIG. 5.— Isotopic mass fractions in the ECSN ejecta relative to their solar values (Lodders 2003) for the unchanged model (upper-left), and the models in which the densities are multiplied by 1.3 (upper-right), 2.0 (lower-left), and 10 (lower-right). ^{48}Ca is indicated by an asterisk in each panel. The normalization band (see the text) is marked in yellow with the medium value indicated by a dashed line in each panel.

SNe or CCSNe. In the limiting case of “ $\rho \times 10$ ”, ^{48}Ca remains the most overproduced isotope, although it is not much increased from the “ $\rho \times 2.0$ ” case. This is a consequence of robust ^{48}Ca production for $\phi < 1$ as proved in Meyer et al. (1996). It is interesting to note that the result in this case resembles to that of high-density SN Ia by Woosley (1997). Isotopes made in α -rich QSE, such as ^{64}Zn , ^{70}Ge , ^{74}Se , and $^{78,86}\text{Kr}$ are all depleted and a reasonable flatness of production factors cannot be seen.

The nucleosynthesis of ^{48}Ca also depends on τ_{exp} . In principle, a slower expansion leads to a later freezeout from NSE and, consequently, leads to α -poor QSE more easily. Such a consequence, however, is not the case in our ECSN model. More slowly expanding matter would be exposed to neutrino absorptions for a longer time, shifting Y_e toward higher values as a result of the α -effect. Such a Y_e increase would compensate the benefits of a slower expansion. One may also consider to increase the ejecta masses where ^{48}Ca is richly produced ($Y_e \approx 0.40$ – 0.42). In fact, fine details of the Y_e - ΔM_{ej} distribution could well depend on the spatial resolution in the simulation or on other factors. It is not plausible, however, to enhance ^{48}Ca without others in our unchanged model. As found in the lower panel of Figure 2, the most overproduced isotope in the range $Y_e < 0.42$ is generally ^{82}Se or ^{84}Kr that already lie on the normalization band (Fig. 5; upper-left).

5. IMPLICATIONS

We studied the nucleosynthesis of ^{48}Ca using the thermodynamic trajectories of a self-consistent 2D explosion model of an ECSN (Janka et al. 2008; Wanajo et al. 2011). Appreciable production of ^{48}Ca was found in α -poor QSE conditions. Comparisons of the mass-integrated yields with the solar abundances show underproduction of ^{48}Ca . This problem would be cured if the entropies in the ejecta were somewhat lower than those in our original model. We conclude, therefore, that ECSNe can be, at least in part, the astrophysical source of ^{48}Ca . The fact that ECSNe can be also associated with the origin of many other isotopes (of light trans-iron species and potentially of weak r-process species, Wanajo et al. 2011) seems encouraging.

Our result also has implications for the interpretation of anomalies of ^{48}Ca found in meteorites (Lee et al. 1978; Moynier et al. 2010; Chen et al. 2011). So far, only hypothetical high-density SNe Ia have been considered as the cause of these anomalies. ECSNe could be, however, an additional source of the anomalies of ^{48}Ca . ECSNe may occur at about one-tenth of the rate of normal CCSNe (Ishimaru & Wanajo 1999; Wanajo et al. 2011), that is, 1–2 events per millennium, which makes them much more common than the rare-class SNe Ia (once in 10,000 years, Woosley 1997). This would be important if the composition of the proto-solar system had been

affected by a single or a few nearby SNe.

More work is needed before final conclusions about the role of ECSNe as production sites of ^{48}Ca can be drawn. In particular, further improvements of ECSN models (e.g., 3D, general relativity, resolution) will be important to elucidate whether appreciable amounts of n-rich ejecta of ECSNe satisfy the α -poor QSE condition

needed for the nucleosynthesis of ^{48}Ca .

S.W. was supported by the JSPS Grants-in-Aid for Scientific Research (23224004). At Garching, support by Deutsche Forschungsgemeinschaft through grants SFB/TR7 and EXC-153 is acknowledged.

REFERENCES

- Asplund, M., Grevesse, N., Sauval, A. J., & Scott, P. 2009, *ARA&A*, 47, 481
- Buras, R., Rampp, M., Janka, H.-T., & Kifonidis, K. 2006, *A&A*, 447, 1049
- Chen, H.-W., Lee, T., Lee, D.-C., Jiun-San Shen, J., & Chen, J.-C. 2011, *ApJ*, 743, L23
- Cyburt, R. H., et al. 2010, *ApJS*, 189, 240
- Hartmann, D., Woosley, S. E., & El Eid, M. F. 1985, *ApJ*, 297, 837
- Hüdepohl, L., Müller, B., Janka, H.-Th., Marek, A., Raffelt, G. G. 2010, *Phys. Rev. Lett.*, 104, 251101
- Ishimaru, Y. & Wanajo, S. 1999, *ApJ*, 511, L33
- Iwamoto, K., Brachwitz, F., Nomoto, K., Kishimoto, N., Umeda, H., Hix, W. R., & Thielemann, F.-K. 1999, *ApJS*, 125, 439
- Janka, H.-Th., Müller, B., Kitaura, F. S., & Buras, R. 2008, *A&A*, 485, 199
- Janka, H.-T., Hanke, F., Hüdepohl, L., Marek, A., Müller, B., & Obergaulinger, M. 2012, submitted to *Prog. Theor. Exp. Phys.*; arXiv1211.1378
- Kitaura, F. S., Janka, H.-Th., & Hillebrandt, W. 2006, *A&A*, 450, 345
- Lee, T., Papanastassiou, D. A., & Wasserburg, G. J. 1978, *ApJ*, 220, L21
- Lodders, K. 2003, *ApJ*, 591, 1220
- McLaughlin, G. C., Fuller, G. M., & Wilson, J. R. 1996, *ApJ*, 472, 440
- Meyer, B. S., Krishnan, T. D., & Clayton, D. D. 1996, *ApJ*, 462, 825
- Meyer, B. S., Krishnan, T. D., & Clayton, D. D. 1998, *ApJ*, 498, 808
- Meyer, B. S., McLaughlin, G. C., & Fuller G. M. 1998, *Phys. Rev. C*, 58, 3696
- Moynier, F., Simon, J. I., Podosek, F. A., Meyer, B. S., Brannon, J., & DePaolo, D. J. 2010, *ApJ*, 718, L7
- Nomoto, K. 1987, *ApJ*, 322, 206
- Poelarends, A. J. T., Herwig, F., Langer, N., & Heger, A. 2008, *ApJ*, 675, 614
- Rampp, M., & Janka, H.-T. 2000, *ApJ*, 539, L33
- Timmes, F. X., Woosley, S. E., & Weaver, T. A. 1995, *ApJS*, 98, 617
- Wanajo, S., Nomoto, K., Janka, H.-T., Kitaura, F. S., Müller, B. 2009, *ApJ*, 695, 208
- Wanajo, S., Janka, H.-T., & Müller, B. 2011, *ApJ*, 726, L15
- Woosley, S. E. & Hoffman, R. D. 1992, *ApJ*, 395, 202
- Woosley, S. E. 1997, *ApJ*, 476, 801